2025 IEEE World Haptics Conference (WHC)
Suwon Convention Center, Suwon, Korea
July 8 ~ 11, 2025

Vibrotactile Sensations in Hands and Fingers Induced by Combined Vibration and Tangential Stimuli on Wrists

Hikaru Saito
University of Tsukuba
Ibaraki, Japan
saito@ah.iit.tskukuba.ac.jp

Taku Hachisu
University of Tsukuba
Ibaraki, Japan
hachisu@iit.tsukuba.ac.jp

***Abstract*—While immersive virtual reality (VR) via head-mounted displays (HMDs) has advanced significantly, reproducing haptic experiences remains a key challenge. Non-contact hand-tracking and wireless HMDs demand haptic feedback to the hands and fingers without direct contact with a device. This study validates a technique that combines vibration and tangential stimuli on the wrists to induce haptic sensations in the hands and fingers. Tangential forces directed toward the elbow increase skin tension, enhancing vibration propagation and creating an illusory sensation localized in more sensitive hand regions. Experimental results show that applying tangential force significantly shifts the perceived vibration toward the fingers, particularly with normal actuation at higher frequencies. These findings inform the design of bracelet-type devices that deliver haptic sensations to the hands and fingers.**

***Index Terms*—Vibrotactile sensation, tangential force, perceived location, wearable technology.**

I. Introduction

Immersive audiovisual experiences through head-mounted displays (HMDs) and stereophonic sound have advanced significantly, yet reproducing haptic experiences of human-object and human-human interactions in virtual environments remains a key challenge. This aspect of virtual reality (VR) technology has garnered increasing attention for its potential to enhance the quality of VR experiences. VR is widely applied in fields such as healthcare, education, and entertainment, enabling users to experience difficult or impossible events in physical environments. Creating haptic interfaces facilitates immersive interactions in a virtual environment, in which users feel plausible existence through the touch [1]–[3]. Hand-based interactions are among the most common activities in daily living [4]–[6], considerable efforts have been dedicated to designing and developing haptic interfaces that provide feedback to the hands and fingers. For instance, handheld controllers like the Meta Quest 3 from Meta integrate built-in vibrotactile actuators to deliver sensory feedback for events occurring in the virtual environment.

With advancements in non-contact hand-tracking capabilities, the demand for non-contact haptic feedback methods is expected to grow. These methods offer users the freedom to interact with objects without holding a controller or pressing the buttons, enhancing interaction flexibility. However, delivering haptic feedback directly to the hands and fingers becomes challenging due to the absence of physical contact with the device or actuator. Additionally, the emergence of wireless HMDs, expanding interaction spaces, highlights the need for mobility-focused solutions.

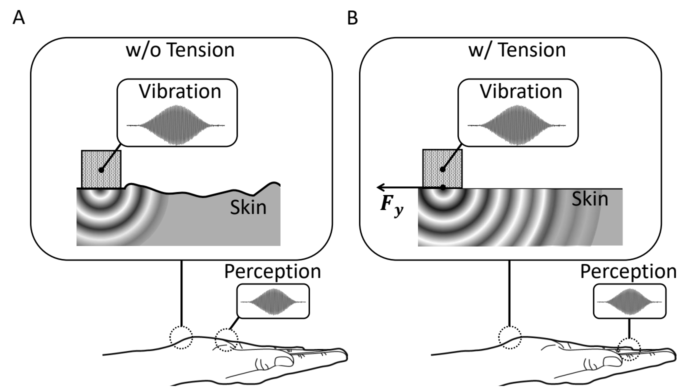

Fig. 1. Vibrotactile sensation delivery to the hands and fingers by combining vibration and tangential stimuli on the wrist: A) Vibration stimuli alone without tangential stimuli — vibrations are rapidly attenuated due to loose skin (low stiffness); B) Combination of tangential and vibration stimuli — vibrations propagate farther due to increased skin tension (high stiffness).

In this study, we present a technique for inducing haptic sensations in the hands and fingers by combining vibration and tangential stimuli applied to the wrists (Fig. 1). Specifically, tangential forces directed toward the elbow increase tension in the wrist-to-finger skin. This increased stiffness propagates the vibration from the wrist to the fingers. Furthermore, leveraging the higher vibrotactile sensitivity of the hand and finger [7] creates an illusory sensation localized in the hand and finger. Because the stimuli consist of vibration and tangential forces applied to the wrists, they can be implemented into a bracelet-type device. This approach enables the delivery of haptic sensations to the hands and fingers without requiring direct device contact with them. An experiment was conducted to evaluate the effects of tangential force, as well as the direction, amplitude, and frequency of vibration, on the perceived location. While implementing the technique in a wearable bracelet device is beyond the scope of this paper, the findings provide valuable insights for designing such devices.

II. Related Work

A. Wearable Haptics

Although grounded haptic devices have been developed to enable haptic interactions in virtual environments [8], their mechanical complexity and high commercial costs may have limited their widespread adoption. To address these challenges, researchers have made significant efforts to develop wearable haptic devices [9]. Vibration stimuli, now commonly integrated into commercial VR controllers and smartwatches, can effectively represent the various events in virtual environments [10]–[12]. Additionally, tangential stimuli, which apply forces to increase skin tension, have been used to deform the skin and induce illusory kinesthetic sensations, such as slippage, friction, and displacement [13]–[15]. These stimuli can be generated using smaller, lighter, and more energy-efficient actuators than those that mechanically affect the musculoskeletal structure of the hands and fingers.

Referred haptics is a concept in which physical stimuli are delivered to body parts distant from those directly involved in the interactions within virtual environments [16]. It represents a form of sensory substitution that extends beyond spatial congruency. Pseudo-haptic feedback can be categorized as a type of referred haptics, wherein stimuli are conveyed through vision (e.g., slowing down a mouse cursor relative to a mouse movement to simulate resistive force sensations in the hand) [17]–[19].

One approach to referred haptics is a bracelet-type device developed by Evan et al., which incorporates a squeezing actuator and six vibrotactile actuators [16]. This device delivers vibrotactile and squeezing stimuli to the wrist to represent the finger contact with virtual objects and the stiffness of these objects, respectively. Users are required to associate the stimuli haptically perceived at the wrists with visually perceived interactions involving the fingers. Another approach is a wearable device developed by Umehara et al., which combines tangential stimuli applied to the wrist skin and vibration stimuli applied to the thumb and index finger [20]. When users interact with virtual objects using their fingers, the device directly stimulates the fingers to convey texture. On the other hand, it indirectly stimulates the wrist skin with tangential forces to simulate the weight sensation of the virtual object, requiring users to interpret wrist-based sensations.

While these studies demonstrate that vibration and tangential forces can be effectively implemented into a bracelet-type device, our approach aims to induce illusory sensations in the hands and fingers through the stimuli applied to the wrists, eliminating the need for users to reference stimuli on other body parts.

B. Vibration Propagation in the Skin

In viscoelastic human skin, vibrations travel from the stimulation site to distant body areas. Hachisu et al. utilized this phenomenon to transmit haptic feedback from one person's wrist (bracelet-type device) to another person by holding hands [21], [22]. Dandu et al. demonstrated spatiotemporal haptic effects, such as expanding and contracting vibrations, using a single actuator through spectral control of vibration propagation in the skin [23]. They exploited the skin's attenuation characteristics as a function of vibration frequency, whereby lower frequencies propagate over longer distances. This method allows a single vibration actuator to produce a range of sensations across the entire finger.

Previous studies have clarified key characteristics of vibration propagation in the skin, such as frequency dependency and three-dimensional propagation patterns, through mechanical measurements [23], [24]. For example, Hachisu et al. conducted mechanical and perceptual experiments to investigate the characteristics of vibration propagation from the wrist to the finger [24]. They found that low-frequency vibrations elicited through tangential actuation are efficiently transmitted, with amplitude varying based on distance, frequency, and actuation direction. Their experiments also highlighted the role of tangential forces in altering skin tension, which affects both mechanical propagation characteristics and perception. These findings underscore the importance of considering both the physical and perceptual aspects of vibration propagation in designing haptic systems.

For simplicity, we consider the skin as a viscoelastic homogeneous medium. The force field $f(\boldsymbol{x}, t)$ can be described by the elastic wave equation:

$$f(\boldsymbol{x}, t) = (-\rho \frac{\partial^2}{\partial t^2} + ((K + \frac{\mu}{3})\nabla)\nabla \cdot + \mu\nabla^2)\boldsymbol{\xi}(\boldsymbol{x}, t), \quad (1)$$

where $\boldsymbol{\xi}(\boldsymbol{x}, t)$ is the time-varying displacement vector field, $\boldsymbol{x}$ is the position, t is time, ρ is the density of the medium, K is the bulk modulus, and μ is the shear modulus [25]. Solutions to Eq. 1 can be expressed as expansions in harmonic plane waves:

$$\boldsymbol{\xi}(\boldsymbol{x}, t) \propto e^{j(\boldsymbol{k} \cdot \boldsymbol{x} - \omega t)}, \quad (2)$$

where $\omega = 2\pi f$ is the angular frequency and $\boldsymbol{k}$ is the wave vector. Prior studies [26], [27] suggest that surface waves in skin in the vibrotactile frequency range (50–200 Hz in this study) are primarily Rayleigh and Love waves, combinations of transverse and longitudinal components, which propagate at speeds similar to those of bulk transverse waves [25], [28]. Thus, the surface wave speed c_S can be approximated as $c_S \approx \sqrt{\mu/\rho}$ [26], [29]. Applying tension T to the viscoelastic medium increases its effective stiffness μ_e, which is reflected in the shear modulus as $\mu_e = \mu_0 + \Delta\mu(T)$, where μ_0 is the baseline shear modulus, and $\Delta\mu(T)$ is the stiffness increase due to T. Empirical observations suggest $\Delta\mu(T) \propto T$. As μ_e increases, c_S also increases accordingly.

Harmonic plane waves (Eq. 2) in the viscoelastic medium may exhibit frequency-dependent damping $D(f)$ [23], [26], [30], which satisfies:

$$\xi_f(\boldsymbol{x}, t) \propto e^{-D(f)\boldsymbol{x}} e^{j(\boldsymbol{k} \cdot \boldsymbol{x} - \omega t)}. \quad (3)$$

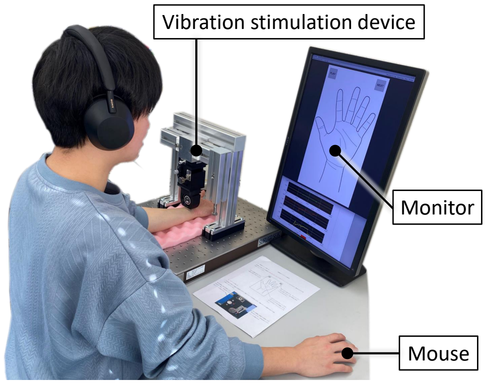

Fig. 2. Experimental setup

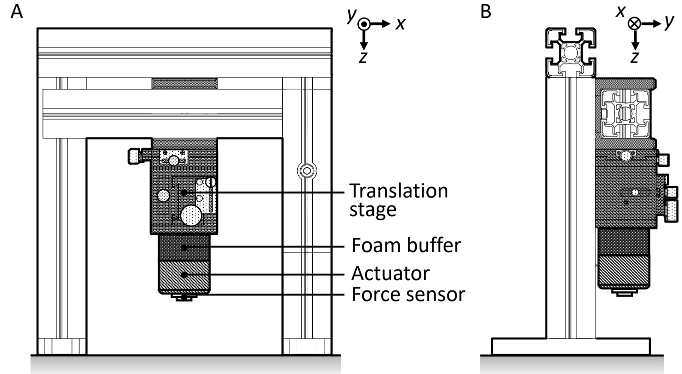

Fig. 3. Vibration stimulation device: A) Front view; B) Side view.

The frequency-dependent damping $D(f)$ in a viscoelastic medium can be expressed as [30]–[32]:

$$D(f) \propto \frac{\mu''}{\mu'} \frac{1}{c_S}, \tag{4}$$

where μ' and μ'' are storage and loss moduli, respectively. When tension increases μ' in addition to the c_S increase, the reduced $D(f)$ results in slower exponential decay according to Eq. 3. This indicates that tension reduces the attenuation of vibrotactile waves, allowing them to propagate further.

III. Experiment

The purpose of this experiment is to investigate the effects of the tangential force, actuation direction, and vibration frequency on the perceived location of vibrotactile stimuli when the actuator is driven on the wrist.

A. Materials

As shown in Fig. 2, the system consisted of a vibration stimulation device, a control board, a host computer, a monitor, a mouse, and headphones.

As shown in Fig. 3, the vibration stimulation device, fixed on a surface plate, consisted of an aluminum frame, a manually adjustable three-axis translation stage (Misumi, XYZLNG60), a foam buffer, a voice-coil actuator (Acouve Laboratory, Vibro-Transducer Vp210) embedded in a 3D-printed polylactic acid case (Ultimaker, Ultimaker S5 Pro), and a three-axis force sensor (Tec Gihan, USL06-H5-50N). Two types of cases were designed to hold the actuator: one for generating vibrations in the normal direction (z-axis in Fig. 3) to the wrist, and the other for generating vibrations in the tangential direction (y-axis in Fig. 3). The foam buffer minimized the vibration propagation from the actuator to the translation stage and the aluminum frame. The three-axis force sensor, with an 18-mm diameter aluminum disk contactor, was attached to the bottom of the case (Fig. 4A). Hereafter, the forces along the z- and y-axes are referred to as the normal force F_z and the tangential force F_y, respectively. The sensor's output was transmitted to the computer via an amplifier (Tec Gihan, DSA-03A) and an analog-to-digital converter (Tec Gihan, DSS300-HR).

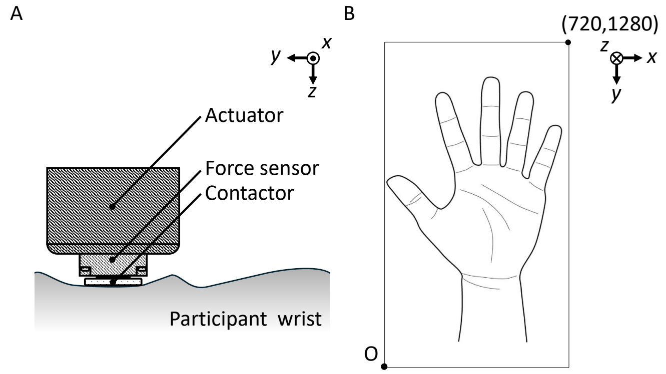

Fig. 4. Details of the setup: A) Illustration of the contact state between the contactor and the wrist skin; B) Coordinate system of the graphical user interface for participants to input perceived locations.

The control board included a microcontroller (Espressif, ESP32-DevKitC) that controlled a digital-to-analog converter (Microchip Technology, MCP4922-E/P, 12 bits) with a 10-kHz refresh rate, which drove the actuator via an audio amplifier (FX-Auido, FX202A/FX-36A PRO). The vibration acceleration $a(t)$ was expressed as:

$$a(t) = w(t) A \sin(2\pi f t),$$
$$w(t) = \begin{cases} 0.5 - 0.5\cos(2\pi \frac{t}{t_0}) & \text{if } 0 \le t \le t_0, \\ 0 & \text{otherwise,} \end{cases} \tag{5}$$

where A is the maximum amplitude, and t_0 is the stimulus duration. The Hanning window $w(t)$ ensured a smooth onset and offset of the stimulus. All parameters were configured via serial communication between the computer and the microcontroller. In this experiment, A was set to 40 m/s^2, f was set to three levels: 50, 100, and 200 Hz, and t_0 was set to 1 s, based on [22], [24].

Frequency-amplitude calibration was performed to maintain a consistent amplitude across the frequencies. The contactor was attached to a medical phantom (Navis, Training Model Skin Suture Model II) under a normal force of 1.5 N (F_z). Figure 5 shows the calibrated vibration acceleration measured by a three-axis accelerometer (Texas Instruments, DRV-ACC16-EVM) mounted between the actuator and the phantom skin, with signals captured by an oscilloscope (Keysight, InfiniiVision MSOX2024A). Although the actuator is uniaxial, negligible but finite accelerations along the axes other than the actuating axis, as well as harmonic components, were observed. Possible reasons include the low assembly accuracy during actuator manufacture, system integration, the system, accelerometer installation, and contact with the phantom skin.

The computer executed the experimental program, displaying a graphical user interface (GUI) on the monitor for participants to play stimuli, input perceived locations (Fig. 4B), view three-axis force data, and receive instructions.

B. Design

We set two levels for the tangential force on the wrist skin (F_y = 0 [N] and 1 [N] $\leq F_y \leq$ 2 [N]), two levels of the actuation direction (normal and tangential directions), and three levels of vibration frequency (50 Hz, 100 Hz, 200 Hz). Consequently, the experiment included 12 types of stimuli. The vibration amplitude A was fixed at 40 m/s^2, and the normal force F_z was maintained to 1 [N] $\leq F_z \leq$ 2 [N]. These values were determined based on prior research [24] and preliminary tests.

Each trial proceeded as follows. First, participants were instructed to play the vibration stimulus using the GUI. Next, they were asked to select the point on the GUI (Fig. 4B) where they perceived the vibration stimulus most strongly. Participants were allowed to replay the stimulus and revise their selection as many times as needed before finalizing their responses. The finalized selection was recorded as xy-plane coordinates.

C. Procedure

Eighteen participants (three females and 15 males) with an average age of 22.3 years participated in the experiment and gave their written, informed consent.

First, the experimenter attached a piece of 10 $\times$ 10-mm double-sided tape to the participants' left wrists. Participants were instructed to place their left forearms under the vibration stimulation device, ensuring that the double-sided tape made contact with the contactor. Next, they were asked to use the translation stage to adjust the contact force to the level specified by the experimenter, using feedback from the three-axial force displayed on the monitor. Participants then were asked to complete 3 trials (3 frequency levels $\times$ 1 repetition) as a practice session to familiarize themselves with the experimental system. After the practice session, the test session was conducted, consisting of 15 trials (3 frequency levels $\times$ 5 repetitions) $\times$ 4 conditions (2 tangential force levels $\times$ 2 actuation direction levels) were conducted as test sessions. The order of frequencies within the 15 trials and the order of actuation directions and tangential forces across the 4 conditions were randomized. To mask audio cues during the test sessions, white noise was delivered to the participants through headphones.

TABLE I
ANOVA TABLE FOR THE PERCEIVED x- AND y-COORDINATES

	x-coordinate			y-coordinate			
Factor	F	p	η^2_G	F	p		η^2_G
TF	0.170	0.686	0.001	6.558	0.020	*	0.012
AD	0.764	0.394	0.003	7.831	0.012	*	0.054
FR	0.645	0.531	0.004	17.16	<0.001	***	0.079
TF×AD	3.348	0.085	0.011	0.430	0.521		0.000
TF×FR	0.762	0.475	0.004	4.710	0.016	*	0.006
AD×FR	0.415	0.664	0.002	9.390	<0.001	***	0.031
TF×AD×FR	0.373	0.691	0.002	1.438	0.252		0.002

* p <0.05, ** p <0.01, *** p <0.001.

D. Analysis

The obtained data consisted of two-dimensional coordinates representing the perceived locations. For each of the 12 stimuli, a 2D Gaussian distribution was fitted to the 90 coordinates (18 participants $\times$ 5 repetitions). This resulted in 12 2D Gaussian distributions, represented by $N(\bar{\boldsymbol{x}}, \boldsymbol{\Sigma})$, where $\bar{\boldsymbol{x}}$ is the mean coordinate and $\boldsymbol{\Sigma}$ is the covariance matrix. These distributions were plotted on the left hand, as illustrated in Fig. 4B.

Additionally, for each participant and each stimulus type, the median coordinate was calculated. Three-way analysis of variance (ANOVA) was performed separately for the x-coordinates and y-coordinates. The within-participant factors were tangential force (TF: w/oTension, w/Tension), actuation direction (AD: Normal, Tangential), and frequency (FR: 50Hz, 100Hz, 200Hz). The significance level was set to 5%. Holm's method was applied for post hoc multiple comparisons when significant effects were detected. It yields a t-value as the test statistic and an adjusted p-value, corrected for multiple comparisons.

E. Results

Figure 6 shows the 2D Gaussian distributions of the perceived locations and the effect of tangential force. The ANOVA results are summarized in Table I. No significant interaction or main effect was found for the perceived x-coordinates, whereas several significant interactions and main effects were found for the perceived y-coordinates.

Focusing on the perceived y-coordinates, Table II presents the multiple comparisons for the significant main effect of FR. Table III shows the simple effects of TF×FR and AD×FR, while Table IV provides the multiple comparisons for those simple effects.

F. Discussion

Although no significant interactions or main effects were identified for the perceived x-coordinates, the three parameters influenced the perceived y-coordinates.

Tangential forces applied to the wrist skin shifted the perceived locations toward the fingers, as expected. This effect

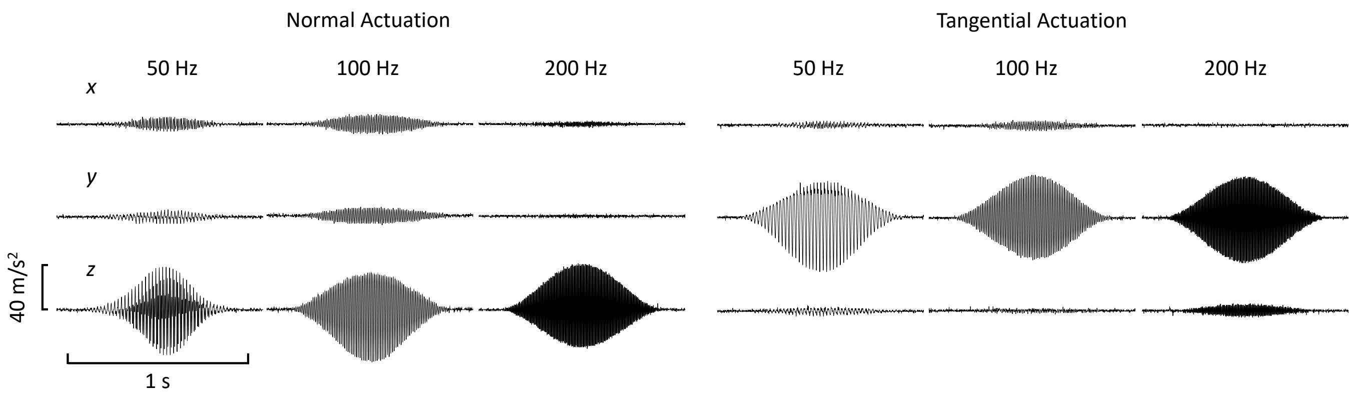

Fig. 5. Six vibrations, with 1-s Hanning window, were used in the experiment: two actuation directions (normal and tangential) × three frequencies (50, 100, and 200 Hz).

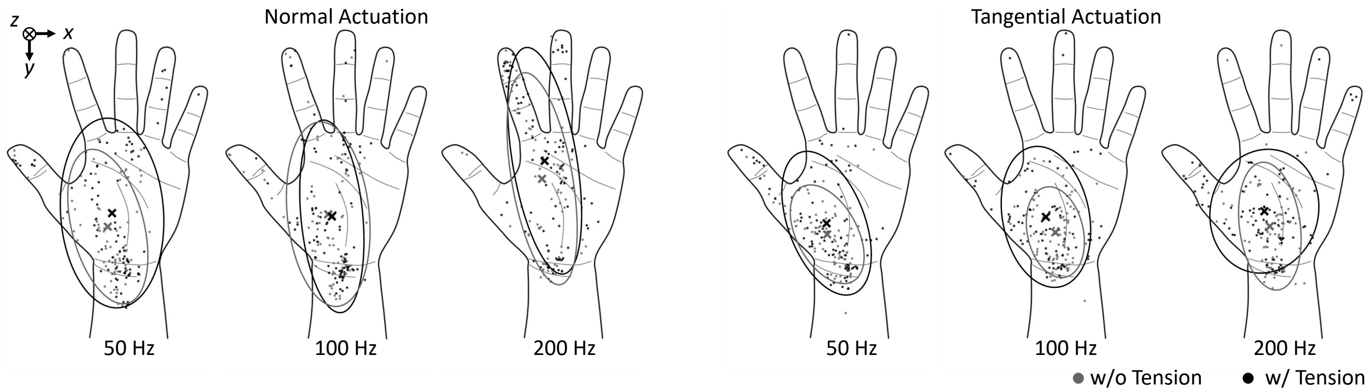

Fig. 6. Two-dimensional Gaussian distributions of the perceived locations for each tangential force, actuation direction, and frequency condition: The dots represent individual perceived locations. The crosses and ellipses are plotted using the means and covariance matrices.

TABLE II
MULTIPLE COMPARISONS FOR MAIN EFFECTS OF FREQUENCY ON THE PERCEIVED y-COORDINATES

Pair	Difference	t	p	
50Hz-100Hz	-16.084	1.121	0.278	
50Hz-200Hz	-110.330	4.273	0.001	**
100Hz-200Hz	-94.246	4.905	<0.001	***

became more pronounced at higher frequencies, according to the multiple comparisons for the simple effect of TF×FR (Table IV). One plausible explanation is that increased skin tension (stiffness) reduced attenuation, as described in Section II-B. To validate the underlying mechanism, future studies could include mechanical measurements of skin stiffness and vibration propagation. While the observed shift in perceived location aligns with our expectations, it is relatively small compared to the effect of actuation direction and frequency. Therefore, exploring greater tangential force levels in subsequent studies may yield additional insights.

Normal actuation caused perceived locations to be farther from the wrist than tangential actuation, with the effect most pronounced at 200 Hz. Notably, several participants reported perceiving the strongest vibrations at the fingertips despite the actuator being attached at the wrist. This finding is consistent with Hachisu et al. [24], who mechanically measured the vibration propagation from the wrist to the fingers. When generated by normal actuation, vibrations attenuate rapidly from the wrist through the palm but appear amplified at the fingertips. In contrast, vibrations generated by tangential actuation attenuate more gradually from the wrist to the palm without a similar amplification at the fingertips.

In this experiment, higher-frequency vibrations (200 Hz) tended to be perceived at locations farther from the wrist, especially when combined with tangential force and normal actuation. Interestingly, prior studies on the mechanical measurements of skin vibration propagation report the opposite trait: higher-frequency vibrations generally damp more quickly [23], [24]. We attribute this discrepancy to the spatial resolution of mechanoreceptors. Low-frequency vibrations are primarily detected by fast-adapting type I mechanoreceptors, which have high spatial resolution, whereas high-frequency vibrations are detected by fast-adapting type Ⅱ mechanoreceptors, which

TABLE III
SIMPLE EFFECTS OF TANGENTIAL FORCE × FREQUENCY AND ACTUATION DIRECTION × FREQUENCY ON THE PERCEIVED y-COORDINATES

Factor	F	p		η_G^2
TF				
FR:50Hz	3.733	0.070		0.017
FR:100Hz	0.174	0.682		0.000
FR:200Hz	9.326	0.007	**	0.029
FR				
TF:w/oTention	11.58	<0.001	***	0.065
TF:w/Tention	16.99	<0.001	***	0.096
AD				
FR:50Hz	2.016	0.174		0.011
FR:100Hz	1.588	0.225		0.020
FR:200Hz	14.76	0.001	**	0.157
FR				
AD:Normal	16.66	<0.001	***	0.127
AD:Tangential	3.877	0.030	*	0.027

TABLE IV
MULTIPLE COMPARISONS FOR SIMPLE EFFECTS OF TANGENTIAL FORCE × FREQUENCY AND ACTUATION DIRECTION × FREQUENCY ON THE PERCEIVED y-COORDINATES

Pair	**Difference**	t	p	
TF:w/oTension				
FR:50Hz-100Hz	-33.70	2.540	0.021	*
FR:50Hz-200Hz	-97.49	3.570	0.007	**
FR:100Hz-200Hz	-63.80	3.417	0.007	**
TF:w/Tension				
FR:50Hz-100Hz	1.528	0.076	0.940	
FR:50Hz-200Hz	-123.2	4.162	0.001	**
FR:100Hz-200Hz	-124.7	5.408	<0.001	***
AD:Normal				
FR:50Hz-100Hz	-22.61	0.974	0.344	
FR:50Hz-200Hz	-176.0	4.372	<0.001	***
FR:100Hz-200Hz	-153.4	4.536	<0.001	***
AD:Tangential				
FR:50Hz-100Hz	-9.556	0.585	0.566	
FR:50Hz-200Hz	-44.61	2.216	0.081	
FR:100Hz-200Hz	-35.06	2.599	0.056	

have lower spatial resolution [33], [34]. Consequently, low-frequency vibrations were more accurately and thus perceived closer to the actual stimulus site on the wrist.

This study presents several opportunities for further research. First, participants in this experiment were asked to select a single point where they perceived the vibration most strongly, but some participants found this difficult because vibrations were felt over a broad area on the hand and fingers. The palm-length distribution of perceived y-coordinates (Fig. 6) supports this observation. We plan to develop a brush-like GUI tool, similar to those used in digital painting software, allowing participants to indicate a perceptual region with varying intensity rather than a single point [35].

Second, subsequent investigations could examine the effects of stimulating different locations on the wrist, such as dorsal and lateral sides, and varying hand postures on the perceived vibration location. These factors likely influence mechanical vibration propagation and, thus, perception. It would also be interesting to explore multiple stimulators to harness wave interference effects.

Third, mechanical measurements of vibration propagation alongside individual differences, such as hand size, skin stiffness, hydration level, and so on, could offer deeper insights into the mechanism of our approach. Understanding these variations would help refine and generalize the method across diverse populations.

Fourth, we aim to implement the findings in a wearable bracelet device. As discussed in Section II-A, prior studies have already demonstrated the technical feasibility of integrating vibration and tangential stimuli into wearable devices. Furthermore, in the context of VR applications, we plan to investigate multimodal effects, where combining visual stimuli may enhance the accuracy and precision of perceived location.

IV. CONCLUSION

In this study, we presented a technique for inducing haptic sensations in the hands and fingers by combining vibration and tangential stimuli applied to the wrist. Tangential forces directed toward the elbow increase tension in the skin between the wrist and fingers, which enhances vibration propagation from the wrist to the fingers. Moreover, leveraging the higher vibrotactile sensitivity of the hands and fingers creates an illusory sensation localized in these areas. To verify this technique, we investigated the effects of tangential force, the actuation direction, and frequency on perceived vibration location. The experimental results showed that applying tangential force significantly shifted the perceived location toward the fingers, particularly when coupled with normal actuation at higher frequencies.

Future work will focus on further elucidating the mechanism of this approach. As discussed, system improvements, such as implementing a brush-like GUI tool for more nuanced perceptual input and mechanical measurements to vibration propagation, would both be valuable.

ACKNOWLEDGMENT

This work was supported by JSPS KAKENHI Grant Numbers JP23K11944 and JP25K03147.

REFERENCES

[1] C. Wee, K. M. Yap, and W. N. Lim, “Haptic interfaces for virtual reality: Challenges and research directions,” *IEEE Access*, vol. 9, pp. 112 145–112 162, 2021.

[2] S. Biswas and Y. Visell, "Haptic perception, mechanics, and material technologies for virtual reality," *Advanced Functional Materials*, vol. 31, no. 39, p. 2008186, 2021. [Online]. Available: https://advanced.onlinelibrary.wiley.com/doi/abs/10.1002/adfm.202008186

[3] T.-H. Yang, J. R. Kim, H. Jin, H. Gil, J.-H. Koo, and H. J. Kim, "Recent advances and opportunities of active materials for haptic technologies in virtual and augmented reality," *Advanced Functional Materials*, vol. 31, no. 39, p. 2008831, 2021. [Online]. Available: https://advanced.onlinelibrary.wiley.com/doi/abs/10.1002/adfm.202008831

[4] L. Reissner, G. Fischer, R. List, P. Giovanoli, and M. Calcagni, "Assessment of hand function during activities of daily living using motion tracking cameras: A systematic review," *Proceedings of the Institution of Mechanical Engineers, Part H: Journal of Engineering in Medicine*, vol. 233, no. 8, pp. 764–783, 2019, pMID: 31132926. [Online]. Available: https://doi.org/10.1177/0954411919851302

[5] Q. Tong, W. Wei, Y. Zhang, J. Xiao, and D. Wang, "Survey on hand-based haptic interaction for virtual reality," *IEEE Transactions on Haptics*, vol. 16, no. 2, pp. 154–170, 2023.

[6] F. Gonzalez, F. Gosselin, and W. Bachta, "Analysis of hand contact areas and interaction capabilities during manipulation and exploration," *IEEE Transactions on Haptics*, vol. 7, no. 4, pp. 415–429, 2014.

[7] A. Adeyemi and M. Sarac, "Comparing the psychophysical capabilities on fingertip and wrist using method of adjustment," *Journal of Emerging Computer Technologies*, vol. 5, no. 1, p. 1–8, 2025.

[8] T. H. Massie, J. K. Salisbury *et al.*, "The phantom haptic interface: A device for probing virtual objects," in *Proceedings of the ASME winter annual meeting, symposium on haptic interfaces for virtual environment and teleoperator systems*, vol. 55, no. 1. Chicago, IL, 1994, pp. 295–300.

[9] C. Pacchierotti, S. Sinclair, M. Solazzi, A. Frisoli, V. Hayward, and D. Prattichizzo, "Wearable haptic systems for the fingertip and the hand: Taxonomy, review, and perspectives," *IEEE Transactions on Haptics*, vol. 10, no. 4, pp. 580–600, 2017.

[10] S. Pabon, E. Sotgiu, R. Leonardi, C. Brancolini, O. Portillo-Rodriguez, A. Frisoli, and M. Bergamasco, "A data-glove with vibro-tactile stimulators for virtual social interaction and rehabilitation," in *10th Annual Intl Workshop on Presence*, 2007, pp. 345–348.

[11] J. Martínez, A. García, M. Oliver, J. P. Molina, and P. González, "Identifying virtual 3d geometric shapes with a vibrotactile glove," *IEEE Computer Graphics and Applications*, vol. 36, no. 1, pp. 42–51, 2016.

[12] E. Giannopoulos, A. Pomes, and M. Slater, "Touching the void: exploring virtual objects through a vibrotactile glove," *International Journal of Virtual Reality*, vol. 11, no. 3, pp. 19–24, 2012.

[13] W. R. Provancher, M. R. Cutkosky, K. J. Kuchenbecker, and G. Niemeyer, "Contact location display for haptic perception of curvature and object motion," *The International Journal of Robotics Research*, vol. 24, no. 9, pp. 691–702, 2005.

[14] K. Minamizawa, S. Fukamachi, H. Kajimoto, N. Kawakami, and S. Tachi, "Gravity grabber: wearable haptic display to present virtual mass sensation," in *ACM SIGGRAPH 2007 emerging technologies*, 2007, pp. 8–es.

[15] B. T. Gleeson, S. K. Horschel, and W. R. Provancher, "Design of a fingertip-mounted tactile display with tangential skin displacement feedback," *IEEE Transactions on Haptics*, vol. 3, no. 4, pp. 297–301, 2010.

[16] E. Pezent, A. Macklin, J. M. Yau, N. Colonnese, and M. K. O'Malley, "Multisensory pseudo-haptics for rendering manual interactions with virtual objects," *Advanced Intelligent Systems*, vol. 5, no. 5, p. 2200303, 2023.

[17] A. Lécuyer, "Simulating haptic feedback using vision: A survey of research and applications of pseudo-haptic feedback," *Presence: Teleoperators and Virtual Environments*, vol. 18, no. 1, pp. 39–53, 2009.

[18] Y. Ujitoko and Y. Ban, "Survey of pseudo-haptics: Haptic feedback design and application proposals," *IEEE Transactions on Haptics*, vol. 14, no. 4, pp. 699–711, 2021.

[19] N. Matsuyama, S. Matsuda, and T. Hachisu, "Can facial expressions induce haptic perception?" *IEEE Transactions on Haptics*, vol. 16, no. 4, pp. 634–639, 2023.

[20] R. Umehara, H. Taguchi, A. Horie, Y. Kamiyama, S. Sakamoto, H. Ishikawa, and K. Minamizawa, "Feeltech wear: Enhancing mixed reality experience with wrist to finger haptic attribution," in *ACM SIGGRAPH 2024 Emerging Technologies*, ser. SIGGRAPH '24. New York, NY, USA: Association for Computing Machinery, 2024. [Online]. Available: https://doi.org/10.1145/3641517.3664395

[21] T. Hachisu and K. Suzuki, "Representing interpersonal touch directions by tactile apparent motion using smart bracelets," *IEEE Transactions on Haptics*, vol. 12, no. 3, pp. 327–338, 2019.

[22] K. Ebina and T. Hachisu, "Interpersonal vibrotactile phantom sensation between hands via actuated bracelets," in *2023 IEEE World Haptics Conference (WHC)*, 2023, pp. 28–33.

[23] B. Dandu, Y. Shao, and Y. Visell, "Rendering spatiotemporal haptic effects via the physics of waves in the skin," *IEEE Transactions on Haptics*, vol. 14, no. 2, pp. 347–358, 2021.

[24] T. Hachisu, G. Reardon, Y. Shao, K. Suzuki, and Y. Visell, "Interpersonal transmission of vibrotactile feedback via smart bracelets: Mechanics and perception," *IEEE Transactions on Haptics*, vol. 17, no. 3, pp. 372–383, 2024.

[25] R. D. Blandford and K. S. Thorne, "Applications of classical physics," *lecture notes, California Institute of Technology*, p. 12, 2008.

[26] L. R. Manfredi, A. T. Baker, D. O. Elias, J. F. Dammann, III, M. C. Zielinski, V. S. Polashock, and S. J. Bensmaia, "The effect of surface wave propagation on neural responses to vibration in primate glabrous skin," *PLOS ONE*, vol. 7, no. 2, pp. 1–10, 02 2012. [Online]. Available: https://doi.org/10.1371/journal.pone.0031203

[27] Y. Shao, V. Hayward, and Y. Visell, "Spatial patterns of cutaneous vibration during whole-hand haptic interactions," *Proceedings of the National Academy of Sciences*, vol. 113, no. 15, pp. 4188–4193, 2016. [Online]. Available: https://www.pnas.org/doi/abs/10.1073/pnas.1520866113

[28] J. Achenbach, *Wave propagation in elastic solids*. Elsevier, 2012.

[29] T. J. Moore, "A survey of the mechanical characteristics of skin and tissue in response to vibratory stimulation," *IEEE Transactions on Man-Machine Systems*, vol. 11, no. 1, pp. 79–84, 1970.

[30] J. Pereira, J. Mansour, and B. Davis, "Dynamic measurement of the viscoelastic properties of skin," *Journal of Biomechanics*, vol. 24, no. 2, pp. 157–162, 1991. [Online]. Available: https://www.sciencedirect.com/science/article/pii/002192909190360Y

[31] K. Mizukami, T. Ikeda, and K. Ogi, "Measurement of velocity and attenuation of ultrasonic guided wave for real-time estimation of cure-dependent anisotropic viscoelastic properties of carbon fiber-reinforced plastics," *Ultrasonics*, vol. 99, p. 105952, 2019. [Online]. Available: https://www.sciencedirect.com/science/article/pii/S0041624X19300757

[32] S. A. Silling, "Attenuation of waves in a viscoelastic peridynamic medium," *Mathematics and Mechanics of Solids*, vol. 24, no. 11, pp. 3597–3613, 2019. [Online]. Available: https://doi.org/10.1177/1081286519847241

[33] R. S. Johansson and Åke B. Vallbo, "Tactile sensory coding in the glabrous skin of the human hand," *Trends in Neurosciences*, vol. 6, pp. 27–32, 1983. [Online]. Available: https://www.sciencedirect.com/science/article/pii/0166223683900115

[34] S. J. Bolanowski Jr, G. A. Gescheider, R. T. Verrillo, and C. M. Checkosky, "Four channels mediate the mechanical aspects of touch," *The Journal of the Acoustical society of America*, vol. 84, no. 5, pp. 1680–1694, 1988.

[35] L. Nummenmaa, E. Glerean, R. Hari, and J. K. Hietanen, "Bodily maps of emotions," *Proceedings of the National Academy of Sciences*, vol. 111, no. 2, pp. 646–651, 2014. [Online]. Available: https://www.pnas.org/doi/abs/10.1073/pnas.1321664111